Identification and control of piezoelectric benders for skin mechanical impedance estimation

Yisha Chen, Michel Amberg, Frédéric Giraud, Vincent Hayward, Betty Lemaire-Semail

Identification and control of piezoelectric benders for skin mechanical impedance estimation

Yisha Chen[1] Michel Amberg[1] Frédéric Giraud[1] Vincent Hayward[2]
Betty Lemaire-Semail[1]
1. Univ. Lille, Arts et Metiers Institute of Technology, Centrale Lille, Junia
ULR 2697 - L2EP, F-59000 Lille, France
2. Sorbonne Université, CNRS, Institut des Systèmes Intelligents et de Robotique, ISIR,
F-75005 Paris, France
Phone: +33 (0)3 62 53 16 34
Email: yisha.chen@univ-lille.fr

Acknowledgements

This research was undertaken within the "Skin Tissue Integrity under Shear" (STINTS) project that has received funding from the European Union's Horizon 2020 research and innovation programme under the Marie Skłodowska-Curie Grant Agreement No. 811965.

This work has been carried out within the framework of IRCICA (CNRS Service and Research Unit 3380) in Lille, France.

Keywords

≪Piezo actuators≫, ≪Motion control≫, ≪Impedance measurement≫, ≪Device application≫, ≪Design≫

Abstract

This paper presents an integrated probe, designed to measure the rheological properties of the skin *in situ*. It includes two piezoelectric bender actuators and strain gauges as sensors. The advantage of the proposed probe is that the measurements of tip force and displacement are accomplished without external devices. A feedback voltage control is applied to control the vibration amplitude of the piezoelectric benders. Through feedback from integrated strain gauges, the displacement control is achieved. As shown in the simulation, the closed-loop system is robust to disturbance and uncertainty. The proposed probe may be used to measure skin mechanical impedance.

Introduction

Pressure ulcers (PUs) are a worldwide health issue. The treatment is usually expensive. PUs at an advanced stage can even be life-threatening [1]. Early diagnosis is recommended to prevent PUs. PUs are associated with the sub-epidermal moisture (SEM) change [2]. Based on this knowledge, devices such as Provizio^{TM} SEM Scanner (Bruin Biometrics, LLC, Los Angeles, CA, USA) have been developed for early detection. SEM Scanners measure electrical capacity resulting from the moisture variation [3]. But the diagnostic specificity of the device is limited to 32.9% [4]. Furthermore, the measurements from SEM Scanners are unitless, which is barely related to the mechanical properties of the skin. Therefore, this research aims to improve the measurement and evaluation of skin properties from a mechanical point of view.

The skin mechanical properties have already been widely studied, with tests of extensometry [5], indentation [6], suction [7] and torsion [8], etc. Research on skin mechanical impedance (MI) for diagnosis

is very limited. In [9], an impedance head was used to measure the MI of the gel tissue model and the skin. The authors discovered that the softer structures (gel with high water content and pitting edema) are characterised by lower MI. However, the impedance head has an inevitable measuring error in acceleration [10]. A piezoelectric actuator working at resonance mode was exploited to identify skin mechanical properties (stiffness and viscosity) under indentation [11]. Nevertheless, the proposed system was not stand-alone, since the measurements of force and indentation depth depended on external devices.

Hence, we propose an integrated probe to estimate skin MI more accurately. It includes piezoelectric actuators and strain gauges. Since MI is sensitive to the moisture level, the proposed MI probe will assist in the early detection of PUs. Our probe is designed based on the methodology presented by Wang et al [12]. In their study, the authors established a dual-pinned structure to stretch skin tangentially. Compared to the dual-pinned structure, the proposed probe is easier to implement with a simple clamped cantilever structure. This paper focuses on the estimation of skin mechanical impedance, where control on displacement is applied.

Mechanical impedance probe design

To perform tangential stretch to the skin, two piezoelectric benders are employed as actuators. Fig. 1a shows the interaction between the proposed probe and the skin. The benders are clamped to each other at one end, working symmetrically. A set of strain gauges are used to measure flexural strain. Fig. 1b depicts the geometry of the MI probe taking one piezoelectric bender as an example. For each bender, we use a pair of strain gauges (RS PRO 632-168) and two resistors, forming a Wheatstone bridge to measure the local strain at the position of strain gauges (l_s). The gauges are placed on the top and bottom surfaces of each bender. In such a way, when bending, one strain gauge is compressed while the other one is extended. The output of the bridge is then amplified by an instrumentation amplifier (INA826).

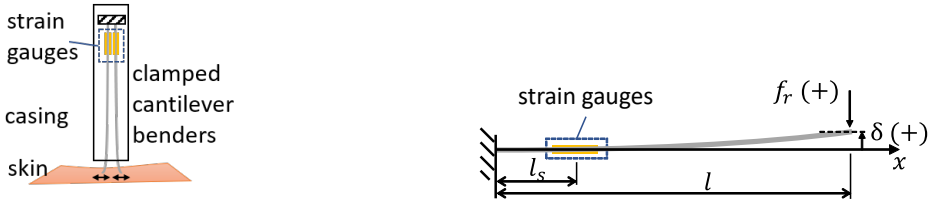

(a) (b)

Fig. 1: (a) System diagram. (b) Geometry of piezoelectric bender with bonded strain gauges. l and l_s indicate the total length of the piezoelectric bender and position centre of strain gauges, respectively.

The two main requirements of the conceived probe are robustness and cost-effectiveness. The dual-pinned structure developed in [12], allows a perfect matching of the actuator's stiffness with skin stiffness. However, a dual-pinned structure is hard to build since it requires a set of pins that have to be positioned with high precision. In contrast, a clamped cantilever structure is easier to integrate, benefiting from recent advances in piezo materials. In Fig. 2, the behaviours of piezoelectric bender from 6 manufacturers are compared. The skin behaviours are depicted as references with an initial gap (initial distance between the two bender tips) of 0.25 mm and 1 mm, respectively. The skin curves were derived from data in [13]. The largest skin displacement is achieved with PB4NB2S from ThorLabs, referring to the intercept points of piezoelectric bender curves with skin curves. Besides, comparing the nominal voltage (denoted as Vmax in Fig. 2), a relatively low voltage is required for PB4NB2S to reach the same displacement. It is obvious that among all the benders, PB4NB2S from ThorLabs is a preferable bender model, considering its high stiffness, large enough deflection when loaded with skin, and less power consumption. Given the effortlessness in mounting, a clamped cantilever structure is recommended.

To drive each bender, a switching amplifier is employed instead of a linear amplifier to reduce power losses. A pulse width modulation is adopted to control the voltage supplied to the bender. The switching frequency is set to 25 kHz to avoid generating audible noise. A half-bridge driver (IR2302) is used to drive the two N-channel power MOSFETs, which form a leg. For the purpose of control, the driving

voltage and the current of the bender are monitored. This current is calculated from the voltage drop through the resistor R_8. Fig. 3a depicts the driving circuits and monitoring circuits. Fig. 3b shows that the driving voltage of the bender is controlled successfully with the designed electrical circuits.

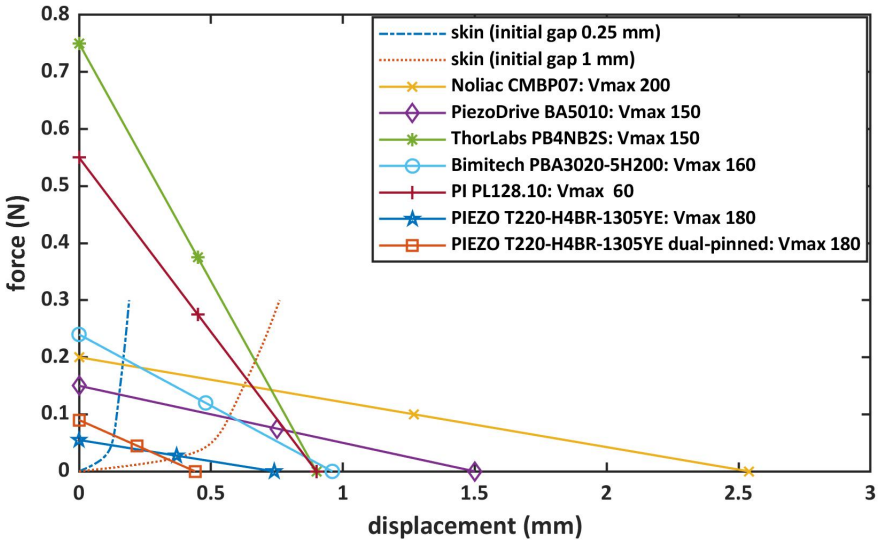

Fig. 2: Piezoelectric bender selection. The parameters used to draw the bender curves were from manufacturers' data sheets, except for PIEZO T220-H4BR-1305YE adopted from [14]. This bender from PIEZO (used to be T220-H4-303Y) was used in [12, 13, 14] and its behaviour with dual-pinned structure was added to compare. Skin curves were derived from data in [13]. Note that the proposed probe has two benders working symmetrically, thus, the displacement value here is the displacement sum of the two benders.

Measuring principle

The mechanical impedance $\bar{z}$ illustrates how much a structure resists to motion when subjected to a harmonic force [15]. It is defined following (1), where $\bar{f}$ is the harmonic force and $\bar{v}$ is the resulting velocity. In our case, $\bar{f}$ is the f_r in harmonic mode. $\bar{v}$ is the first order derivative of δ.

$$\bar{z} = \frac{\bar{f}}{\bar{v}} \tag{1}$$

From the constituent equation of cantilever piezoelectric bender [16], tip displacement δ can be determined from a linear superposition of the supplied voltage V and the external force f_r (acting at the bender tip, perpendicular to the beam). Referring to Fig. 1b, in static state, this relationship is expressed as (2):

$$\delta = S_{dv}V - S_{df}f_r \tag{2}$$

where S_{dv} and S_{df} represent the sensitivity of tip displacement to supplied voltage and external force, respectively and the sign convention is illustrated in Fig. 1b. The tip force and displacement should be measured to obtain the mechanical impedance. In (2), the supplied voltage V is already known, but to further obtain f_r and δ at the same time, one more formula is needed. Hence, strain gauges are utilised.

The strain gauges measure the average flexural strain g along its length. Subjected to voltage and external force, g is determined by (3) [17]:

$$g = S_{gv}V - S_{gf}f_r \tag{3}$$

Similar to (2), S_{gv} and S_{gf} in (3) represent the sensitivity of g to V and f_r, respectively.

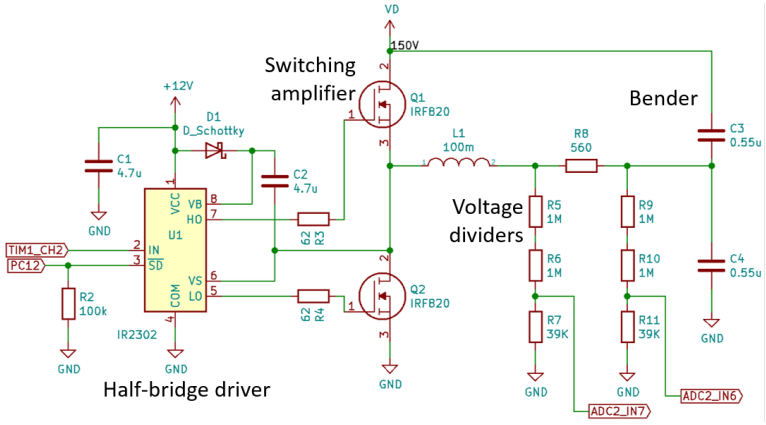

(a)

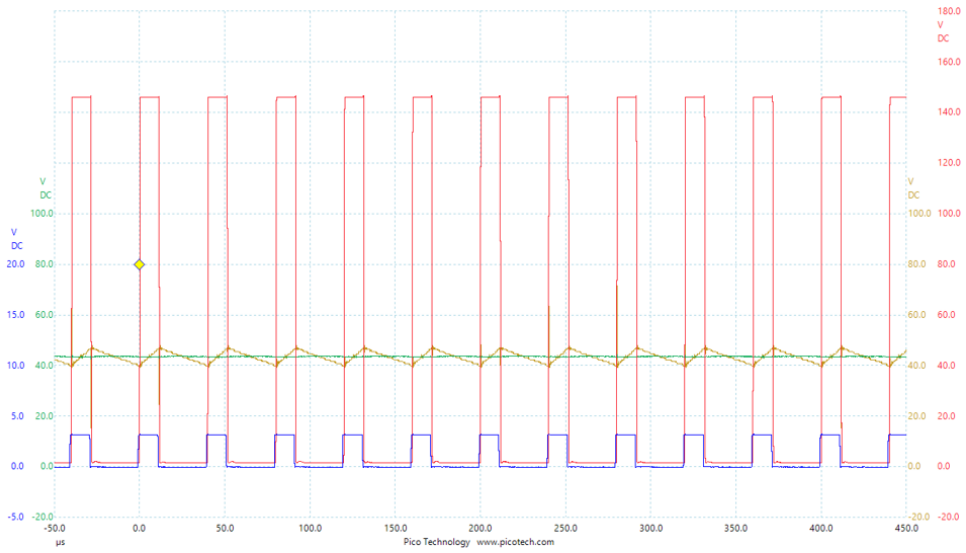

(b)

Fig. 3: (a) Electrical scheme of driving circuits and monitoring circuits for one bender. The bender is represented by its capacitance ($2 \times 0.55\mu$F). (b) Example of pulse width modulation. The blue curve is the pulse signal given to the half-bridge driver. The red curve is the output of the switching amplifier (the leg). The yellow curve is the voltage before the damping resistor (R_8). The green curve is the voltage after R_8, i.e., the driving voltage of the bender.

From a global view of the designed electromechanical system, the bender driving voltage V and the output of strain gauges g are measured and may be considered as the inputs. The outputs of this system are the tip displacement δ and force f_r. Consequently, the tip displacement and force of piezoelectric bender can be estimated from (V, g), given by (4)

$$\begin{bmatrix} \widehat{\delta} \\ \widehat{f_r} \end{bmatrix} = \begin{bmatrix} G_{dv} & G_{dg} \\ G_{fv} & G_{fg} \end{bmatrix} \begin{bmatrix} V \\ g \end{bmatrix} \tag{4}$$

where G_{dv}, G_{dg}, G_{fv}, G_{fg} are the gains to be identified. Comparing (4) to (2) and (3), we obtain (5)

$$\begin{cases} G_{dv} = S_{dv} - S_{df}\frac{S_{gv}}{S_{gf}}, G_{dg} = \frac{S_{df}}{S_{gf}} \\ G_{fv} = \frac{S_{gv}}{S_{gf}}, G_{fg} = -\frac{1}{S_{gf}} \end{cases} \tag{5}$$

Hence, the identification of the gains can be achieved by identifying the sensitivities, i.e., S_{dv}, S_{df}, S_{gv}, and S_{gf}. In this section, an estimator on tip displacement and force is developed.

System identification and model

To estimate tip displacement and force, sensitivities related to (2) and (3) have been identified. The free stroke (where $f_r = 0$) and blocking force (where $\delta = 0$) of the piezoelectric bender have been measured with a laser sensor and an external force sensor (FSS low profile force sensor), separately. Fig. 4 shows the measuring results with a sinusoidal driving voltage at 1 Hz, full scale. Note that the full-scale voltage here is slightly less than the nominal value for the sake of protection. Hysteresis exists between free stroke and driving voltage, which is captured by the signal from strain gauges. When the bender is blocked, no hysteresis appears between blocking force and driving voltage, neither in the output of strain gauges. These phenomena lead us to a hypothesis that the hysteresis is displacement-dependent considering the presence of external force in addition to the driving voltage.

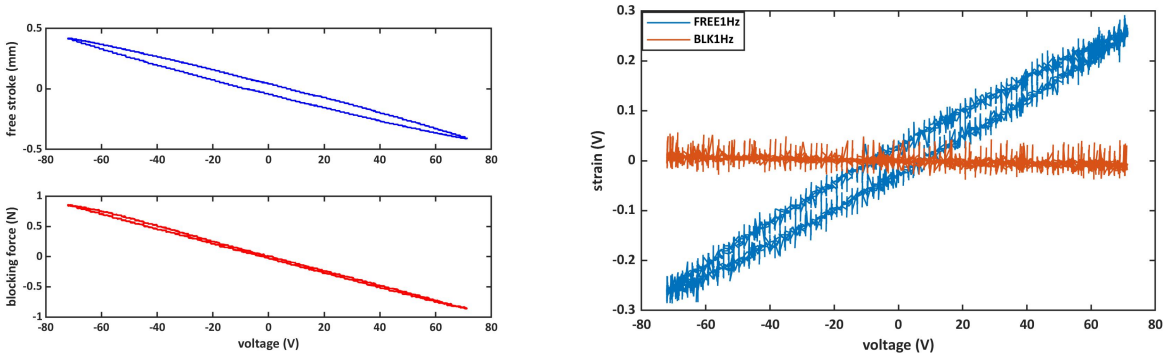

(a) (b)

Fig. 4: (a) Free stroke and blocking force against driving voltage. (b) Strain gauge signal against driving voltage when the bender tip is free and blocked, respectively.

The piezoelectric bender can be modelled by (6) [18]:

$$M\ddot{\delta} + D\dot{\delta} + K\delta = NV - f_r \tag{6}$$

where M, D, K, and N are the mass, damping, stiffness, and force factor of the piezoelectric bender, respectively.

As the proposed probe operates in quasi-static condition, (6) can be simplified as (7)

$$\delta = \frac{N}{K}V - \frac{1}{K}f_r \tag{7}$$

Comparing (7) to (2), we obtain $K = \frac{1}{S_{df}}$. N can be identified from blocking tests, with $N = \frac{f_r}{V}|_{\delta=0}$. To design the controller, the piezoelectric bender is modelled as a first-order system, considering D and K. D has been identified through a frequency sweep with a low amplitude driving voltage. The results of system identification are summarised in Table I. The negative sign is related to the mechanical mounting of the two benders and the sign convention defined in Fig. 1b.

Table I: Results of system identification

D (N·s/mm)	K (N/mm)	N (N/V)
0.0884×10^{-3}	2.075	-0.0118

System control and simulation

Skin is known as a *non-homogeneous, anisotropic, non-linear viscoelastic multi-component* material [19]. To ensure the repeatability and comparability of the measurements, closed-loop control is required. As discussed in the previous section, the hysteresis behaviour depends on displacement. Thus, the vibration amplitude of the piezoelectric bender is controlled. Fig. 5 presents the feedback control scheme on bender tip displacement δ. The piezoelectric bender is modelled by a first-order system. To follow the reference displacement δ_{ref}, a PI controller is designed to tune the driving voltage V. System simulation is implemented with Matlab Simulink, using the parameters from system identification (Table I). In practice, the feedback signal is the estimated $\widehat{\delta}$.

Fig. 6 shows the closed-loop response of the system presented in Fig. 5. The reference signal δ_{ref} is a sine waveform at 1 Hz, with an amplitude of 0.1 mm. The external force f_r is derived from a linearised viscoelastic skin model proposed in [13]. Moreover, non linearity (hysteresis) is added to the piezoelectric bender model. The performance of the controller is evaluated by the relative peak-to-peak error between system output δ and the reference δ_{ref}. To evaluate the accuracy of the estimator, $\widehat{\delta}$ and δ are compared. Results show that both for controller and estimator, the relative peak-to-peak errors are 5%. It is confirmed that the system can reject the disturbance and uncertainty. The error in estimation can be explained by the linear modelling of strain gauges in simulation (referring to (3)). In reality, strain gauges capture the hysteresis phenomena of the piezoelectric bender.

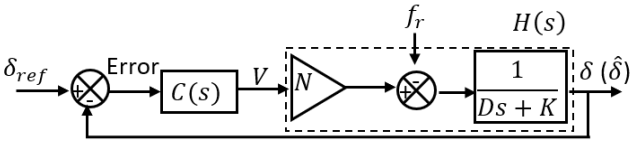

Fig. 5: Closed-loop control of the vibration amplitude. $C(s)$ is the controller and $H(s)$ is the process.

With the skin model and skin parameters provided in [13], the frequency response of skin over 1 Hz–1000 Hz is studied through simulation. To introduce skin changes, one of the skin parameters (viscosity η_2) is varied. The diversity of mechanical impedance of different skins is demonstrated in Fig. 7. Below 20 Hz, MI magnitude decreased obviously for the skin with a lower η_2. This finding is in good agreement with [9], regarding that low viscosity corresponds to high water content. In [20], higher sub-epidermal moisture is associated with PUs. Hence, a lower mechanical impedance is expected for skins at risk of PUs. It is observed that the MI phase can also imply changes in skin condition. Therefore, the magnitude and the phase of mechanical impedance can be used for skin characterising. Additionally, the frequency range can be narrowed to 1 Hz–100 Hz or less, as skins' behaviour changed significantly within this range.

Discussion

This research is inspired by the work in [12]. Our contributions here are twofold. On one hand, we simplified the mechanical structure of the probe. On the other hand, we achieved a robust control on tip

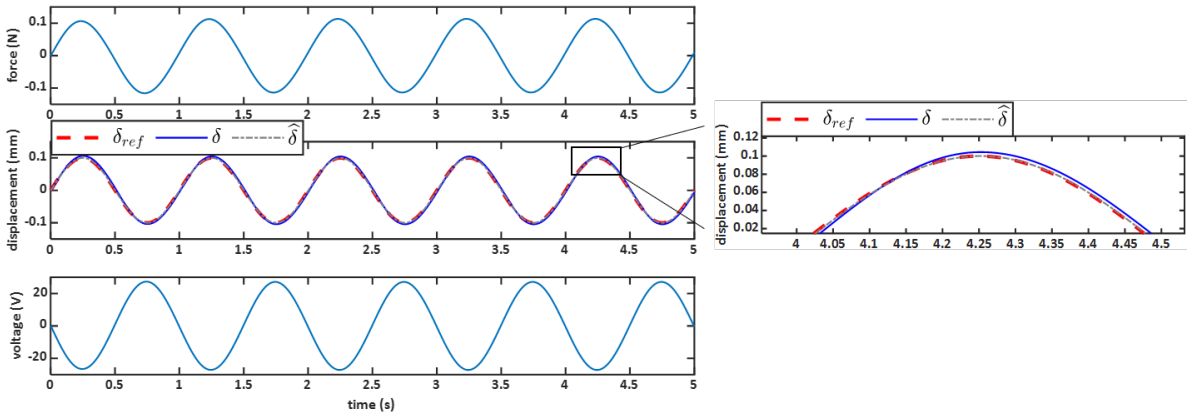

Fig. 6: Closed-loop response of the system at 1 Hz in simulation. The external force is given by a linearised skin model. Top: external force (f_r); middle: reference input (δ_{ref}), output of the system (δ), and estimated value ($\widehat{\delta}$); bottom: output of the controller (V).

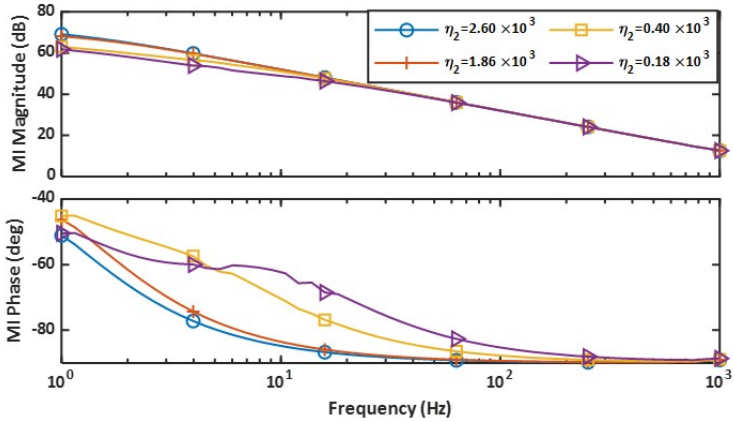

Fig. 7: Mechanical impedance of skin with different viscosities (η_2). Skin parameters from [13].

displacement without external device needed. In [13], control was implemented with an external laser sensor. In our case, the control is achieved with a feedback signal given by the internal estimator we developed. This feature makes the system easy to be compact.

As seen in Fig. 5, the driving voltage is tuned to control the behaviour of the piezoelectric bender. Compared to charge control, the electrical circuit is less complicated for feedback voltage control [21].

The nonlinearity (hysteresis) of piezoelectric ceramics is a common issue, which affects the accuracy of positioning [21]. For the proposed system, the signals from strain gauges reflect the hysteresis behaviour, which contributes to the accurate estimation of tip displacement with (4).

Conclusion

An electromechanical probe, based on piezoelectric benders and strain gauges, is proposed to measure the mechanical properties of skin in situ. With this device, skin displacement and force are obtained simultaneously without external devices. Through an internal estimator, the control on vibration amplitude is accomplished. Simulation results show that the closed-loop system is robust to reject low-frequency load. Currently, we are working on the implementation of the real system.

Skin responses in simulation indicate that mechanical impedance can be used to evaluate skin conditions. Specifically, a low impedance magnitude is expected for skin at risk of pressure ulcers. This finding needs to be confirmed with *in vivo* tests.

References

[1] Dealey C., Posnett J., and Walker A.: The cost of pressure ulcers in the United Kingdom, Journal of Wound Care, Aug. 2013, doi: 10.12968/jowc.2012.21.6.261.

[2] Moore Z., Patton D., Rhodes S. L., et al.: Subepidermal moisture (SEM) and bioimpedance: a literature review of a novel method for early detection of pressure-induced tissue damage (pressure ulcers).International Wound Journal,14(2):331–337, 2017.

[3] Gefen A. and Ross G.: The subepidermal moisture scanner: the technology explained.Journal of Wound Care, 29(Sup2c):S10–S16, February 2020

[4] Okonkwo H., Bryant R., Milne J., et al.: A blinded clinical study using a subepidermal moisture biocapacitance measurement device for early detection of pressure injuries, Wound Repair & Regeneration, vol. 28, no. 3, pp. 364–374, 2020, doi: 10.1111/wrr.12790.

[5] Jacquet E., Joly S., Chambert J., et al.: Ultra-light extensometer for the assessment of the mechanical properties of the human skin in vivo, Skin Research & Technology, vol. 23, no. 4, pp. 531–538, 2017, doi: 10.1111/srt.12367.

[6] Pailler-Mattei C., Bec S., and Zahouani H.: In vivo measurements of the elastic mechanical properties of human skin by indentation tests, Medical Engineering & Physics, vol. 30, no. 5, pp. 599–606, Jun. 2008, doi: 10.1016/j.medengphy.2007.06.011.

[7] Luebberding S., Krueger N., and Kerscher M.: Mechanical properties of human skin in vivo: a comparative evaluation in 300 men and women, Skin Research & Technology, vol. 20, no. 2, pp. 127–135, 2014, doi: 10.1111/srt.12094.

[8] Blair M. J., Jones J. D., Woessner A. E., et al.: Skin structure-function relationships and the wound healing response to intrinsic aging, Advances in Wound Care, vol. 9, no. 3, pp. 127–143, 2020, doi: 10.1089/wound.2019.1021.

[9] Mridha M. and Ödman S.: Characterization of subcutaneous edema by mechanical impedance measurements, Journal of Investigative Dermatology, vol. 85, no. 6, pp. 575–578, Dec. 1985, doi: 10.1111/1523-1747.ep12283588.

[10] Brownjohn J. M. W., Steele G. H., Cawley P., et al.: Errors in mechanical impedance data obtained with impedance heads[J]. Journal of Sound and Vibration, 1980, 73(3): 461-468.

[11] Sienkiewicz L., Ronkowski M., Kostro G., et al.: Identification of the mechanical properties of the skin by electromechanical impedance analysis of resonant piezoelectric actuator[C]//IECON 2013-39th Annual Conference of the IEEE Industrial Electronics Society. IEEE, 2013: 3940-3945.

[12] Wang Q., Kong L., Sprigle S., et al.: Portable gage for pressure ulcer detection, in 2006 International Conference of the IEEE Engineering in Medicine and Biology Society, Aug. 2006, pp. 5997–6000, doi: 10.1109/IEMBS.2006.260070.

[13] Wang Q. and Hayward V.: In vivo biomechanics of the fingerpad skin under local tangential traction, Journal of Biomechanics, vol. 40, no. 4, pp. 851–860, Jan. 2007, doi: 10.1016/j.jbiomech.2006.03.004.

[14] Wang Q. and Hayward V.: Biomechanically optimized distributed tactile transducer based on lateral skin deformation, International Journal of Robotics Research, vol. 29, no. 4, pp. 323–335, Apr. 2010, doi: 10.1177/0278364909345289.
[15] Sabanovic A. and Ohnishi K.: Interactions and constraints, in Motion Control Systems, John Wiley & Sons, 2011.
[16] Ballas R. G., Schlaak H. F., and Schmid A. J.: The constituent equations of piezoelectric multilayer bending actuators in closed analytical form and experimental results, Sensors and Actuators A: Physical, vol. 130–131, pp. 91–98, Aug. 2006, doi: 10.1016/j.sna.2005.11.034.
[17] Seethaler R., Mansour S. Z., Ruppert M. G., et al.: Position and force sensing using strain gauges integrated into piezoelectric bender electrodes, Sensors & Actuators A: Physical, p. 112416, Nov. 2020, doi: 10.1016/j.sna.2020.112416.
[18] Giraud F. and Giraud-Audine C.: Piezoelectric actuators: Vector control method. Elsevier, 2019.
[19] Maurel W., Thalmann D., Wu Y., et al: Biomechanicalmodels for soft tissue simulation, volume 48. Springer, 1998.
[20] Bates-Jensen B. M., McCreath H. E., Pongquan V.: Sub-epidermal moisture is associated with early pressure ulcer damage in nursing home residents with dark skin tones: Pilot findings[J]. Journal of wound, ostomy, and continence nursing: official publication of The Wound, Ostomy and Continence Nurses Society, 2009, 36(3): 277.
[21] Ronkanen P., Kallio P., Koivo H. N.: Current control of piezoelectric actuators with power loss compensation[C]//IEEE/RSJ International Conference on Intelligent Robots and Systems. IEEE, 2002, 2: 1948-1953.